

One laser pulse generates two photoacoustic signals

Fei Gao^{1,†,*}, Xiaohua Feng^{1,†}, Yuanjin Zheng^{1,*}

¹*School of Electrical and Electronic Engineering, Nanyang Technological University*

[†]Authors contributed equally to this work

*Corresponding to: fgao1@e.ntu.edu.sg; yjzheng@ntu.edu.sg

Abstract:

Photoacoustic sensing and imaging techniques have been studied widely to explore optical absorption contrast based on nanosecond laser illumination. In this paper, we report a long laser pulse induced dual photoacoustic (LDPA) nonlinear effect, which originates from unsatisfied stress and thermal confinements. Being different from conventional short laser pulse illumination, the proposed method utilizes a long square-profile laser pulse to induce dual photoacoustic signals. Without satisfying the stress confinement, the dual photoacoustic signals are generated following the positive and negative edges of the long laser pulse. More interestingly, the first expansion-induced photoacoustic signal exhibits positive waveform due to the initial sharp rising of temperature. On the contrary, the second contraction-induced photoacoustic signal exhibits exactly negative waveform due to the falling of temperature, as well as pulse-width-dependent, signal amplitude which is caused by the concurrent heat accumulation and thermal diffusion during the long laser illumination. A simple analytical model is derived to describe the generation of the dual photoacoustic pulses, incorporating Gruneisen saturation and thermal diffusion effect, which is experimentally proved. The LDPA nonlinear effect also enables many potential applications using a low-cost laser diode system.

Photoacoustic (PA) technique has been attracting wide range of research interest in recent decade for biomedical imaging. Due to the hybrid merit of optical absorption and ultrasound detection, PA technique has successfully overcome the long-standing challenge of optical diffusion in deep scattering medium, achieving sensitive optical absorption contrast and scalable spatial resolution [1-7]. To induce strong enough PA signal, high-power nanosecond pulsed laser is usually utilized as the light source [8-11]. With ultrashort laser pulse (e.g. 1~10 ns), both thermal and stress confinements are satisfied to obtain optimized conversion efficiency from light absorption to ultrasound emission. When one pulse is illuminated on the target, one PA signal could be induced through transient absorption, heating and thermal expansion. However, there is no literature reporting using one laser pulse to generate two nonlinearly correlated PA signals.

We report a PA technique based on long laser pulse induced dual PA (LDPA) nonlinear effect, which, for the first time, enables two nonlinearly correlated PA signals' generation from one laser illumination. To induce two PA signals from one laser pulse, two sharp laser intensity transitions are required. Therefore we employ square-profile laser illumination, rather than Gaussian-profile of conventionally used laser source. Due to the sharp rising and falling edges of the square laser pulse, two PA signals originating from thermal expansion and contraction respectively, are expected to be generated. In addition, the laser pulse width should be long enough (larger than stress confinement time), so that the two expansion-induced and contraction-induced PA signals could be separated in time domain. It is also expected that the two PA signals should show phase-inverted (180 degree difference) waveforms due to the separate expansion and contraction effects. More interestingly, the two PA signals should exhibit different signal strengths that may vary with different laser pulse width, which are caused by the concurrent heat accumulation and diffusion during the long laser pulse illumination (thermal confinement is not strictly met). Being clearly distinct from other reported thermal nonlinear PA technique that only happens when laser fluence exceeds a threshold value [12-14], the proposed LDPA nonlinear effect could be observed with low-power laser diode and applied in much broader range of applications. The nonlinearity of the LDPA effect could immediately enables several interesting applications, such as axial super-resolution PA imaging [15], and PA-guided optical focusing [16]. In this paper, an analytical model is derived to describe the proposed LDPA nonlinear

effect, and proof-of-concept experiments are performed to demonstrate its feasibility. The potential applications utilizing the LDPA effect are also discussed.

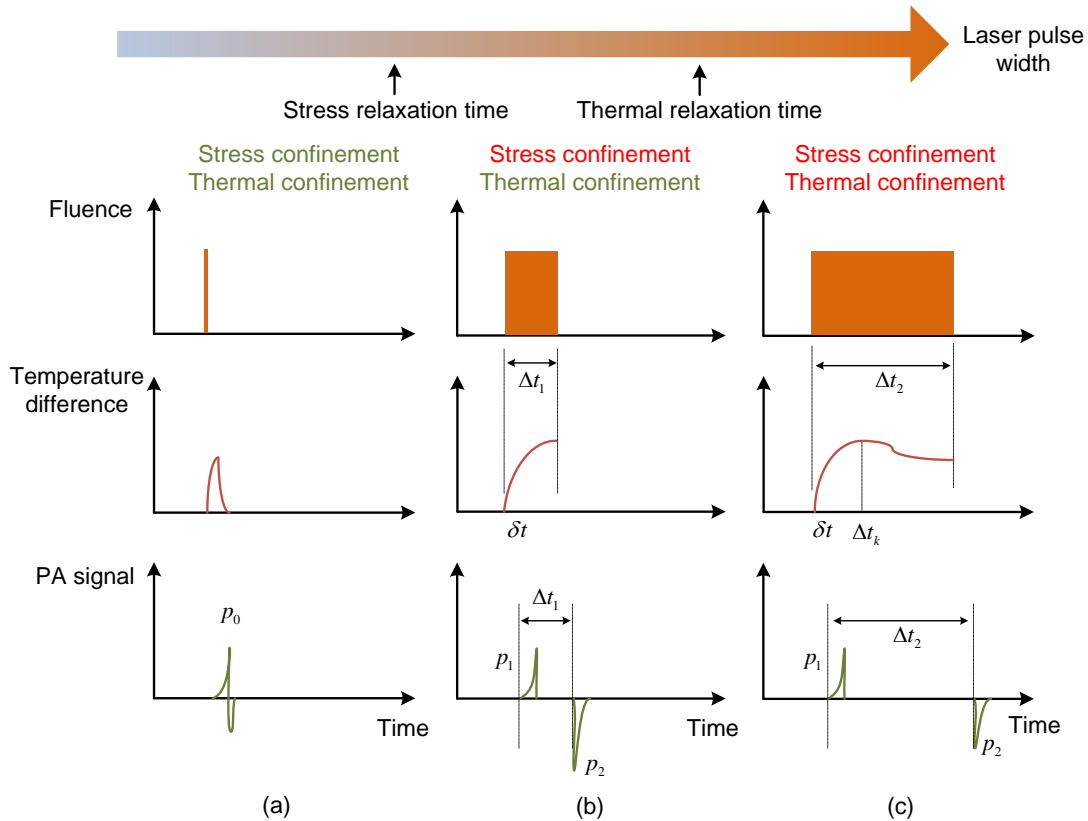


Fig. 1. The fluence pattern, temperature change and PA signal waveform of (a) conventional short laser pulse induced PA effect with both stress and thermal confinements satisfied; (b) long laser pulse induced dual PA nonlinear effect with only thermal confinement satisfied, and (c) even longer laser pulse without thermal confinement.

Conventionally the short laser pulse with nanosecond pulse-width is used to induce transient temperature change in the optical absorber with both stress and thermal confinements, and a dipolar PA signal is generated following the thermoelastic expansion and contraction (Fig. 1(a)). To further increase the laser pulse-width to be larger than stress relaxation time ($\Delta t_1 > \tau_s = d/v$, d is the PA source diameter, v is the acoustic velocity), the single dipolar PA signal is gradually separated into two independent but correlated PA signals. The first pulse is expansion-induced positive PA signal p_1 , the second pulse is contraction-induced negative PA signal p_2 with exactly inverted waveform (Fig. 1(b)). The first PA signal is generated immediately after the

sharp temperature rise of the laser illumination, which is related with the light irradiation ϕ (W/cm^2) within short rising period δt . The analytical expression of p_1 is similar with the conventional short laser pulse induced PA:

$$p_1 = \Gamma_0 \eta_{th} \mu_a \phi \delta t \quad (1)$$

where Γ_0 is the Gruneisen coefficient at the ambient temperature. η_{th} is the conversion efficiency from heat to pressure, and μ_a is the optical absorption coefficient.

On the other hand, the second PA signal p_2 could exhibit larger amplitude than the first one, which could be caused by more light energy deposition in the object, and higher Gruneisen coefficient (thermal expansion coefficient increased) due to the temperature rise of the object (Fig. 1(b)). However, when the laser pulse-width is further increased to larger than thermal relaxation time ($\Delta t_2 > \tau_{th} = d^2/\alpha$, α is the thermal diffusivity of the object), the amplitude of p_2 will be close to the amplitude of p_1 , which is due to the significant thermal diffusion during the long laser illumination. Incorporating the considerations above, the analytical expression of p_2 could be derived as:

$$p_2 = \left\{ \overbrace{\Gamma_0 + b \eta_{th} \mu_a \tau_{th} \phi \left[1 - \left(1 + \frac{\Delta t}{\tau_{th}} \right) \exp \left(-\frac{\Delta t}{\tau_{th}} \right) \right]}^{\text{Gruneisen saturation term}} \right\} \eta_{th} \mu_a \phi \delta t + \Gamma_0 \eta_{th} \mu_a \overbrace{\phi \Delta t \exp \left(-\frac{\Delta t}{\tau_{th}} \right)}^{\text{Fluence Thermal diffusion}} \quad (2)$$

where b is the coefficient relating the absorbed thermal energy to the Gruneisen parameter change, and Δt is the laser pulse-width. Compared with Eq. (1) of the first conventional linear PA, the second PA signal p_2 shows nonlinearity governed by three terms in Eq. (2). The Gruneisen saturation term describes the object's temperature rising and saturation due to heat accumulation during one laser pulse illumination. The light fluence term is linearly increasing with laser pulse-width, and the thermal diffusion term is exponentially decaying according to Newton's law of cooling due to temperature difference. The Gruneisen saturation term is derived

by the time integration of heat deposition and diffusion ($b\eta_{th}\mu_a\phi\int_0^{\Delta t}t\exp\left(-\frac{t}{\tau_{th}}\right)dt$). The analysis of the second nonlinear PA signal could be simplified under three cases:

1) $\Delta t \ll \tau_{th}$, $\exp\left(-\frac{\Delta t}{\tau_{th}}\right) \approx 1$, and ϕ is large using high-power pulse laser

For this case as shown in Fig. 1(b), thermal diffusion is neglected within short period. However, the Gruneisen saturation is significant due to the large light intensity ϕ . Then Eq. (2) could be simplified as:

$$p_2 = \Gamma_0 \eta_{th} \mu_a \phi (\delta t + \Delta t) + (b \eta_{th} \mu_a \phi \Delta t) \eta_{th} \mu_a \phi \delta t \quad (3)$$

This case is similar with the thermal nonlinear PA technique using two consequent short high-power laser pulses, where the second PA pulse is nonlinearly enhanced by the Gruneisen relaxation effect induced by the first pulse's heating [15, 16].

2) $\Delta t \geq \tau_{th}$, and ϕ is small using low-power laser diode

For this case as shown in Fig. 1(c), the thermal diffusion is becoming more significant with increasing laser pulse width. In addition, due to the low light intensity generated by low-power laser source, such as laser diode, the heat accumulation as well as the Gruneisen saturation term could be neglected during the laser illumination. The Eq. (2) could be simplified as:

$$p_2 = \Gamma_0 \eta_{th} \mu_a \phi \left[\delta t + \Delta t \exp\left(-\frac{\Delta t}{\tau_{th}}\right) \right] \quad (4)$$

This is the case of using low-power laser diode, where the second nonlinear PA signal will experience a short-period PA signal increase due to dominant fluence accumulation, then a long-period PA signal decrease due to dominant thermal diffusion. The most straightforward way to characterize this PA nonlinearity is to sweep the pulse width Δt and analyze the amplitude of p_2 .

The key pulse width $\Delta t_k = \tau_{th}$ when $\frac{\partial p_2}{\partial \Delta t} = 0$ is the turning point from amplitude increase to decrease as shown in Fig. 1(c), which could be used as the nonlinear characterization feature.

To make it simpler without sweeping the laser pulse width, another way is to calculate the nonlinear ratio R_{nl} between the second nonlinear PA p_2 and the first linear PA p_1 :

$$R_{nl} = \frac{p_2}{p_1} = 1 + \frac{\Delta t}{\delta t} \exp\left(-\frac{\Delta t}{\tau_{th}}\right) \quad (5)$$

It is worth noting that R_{nl} is only determined by the thermal relaxation time of the optical absorber at a fixed laser pulse width. Compared with the conventional linear PA technique shown in Eq. (1) that usually suffers from unknown fluence and conversion efficiency variations in real applications, the proposed nonlinear ratio is intrinsically immune to those variations and provides thermal diffusivity contrast beyond the optical absorption contrast. This feature immediately enables sensitive and reliable detection of optical absorber by its thermal diffusivity properties, which has the potential in glucose [17], lipid detection [18], and contrast-enhanced PA imaging using nanoparticles [19, 20].

As mentioned before, although the key pulse width $\Delta t_k = \tau_{th}$ could provide the maximum amplitude of p_2 and nonlinear ratio R_{nl} from a specific target, it may not be the optimum laser pulse width when it is applied to real sensing/imaging applications with both target and background. Suppose the target and background exhibit thermal relaxation times τ_{th} and τ_{th_b} , and in order to maximize the sensitivity and contrast to differentiate the target from the background, the nonlinear ratio difference could be derived as:

$$\Delta R_{nl} = R_{nl} - R_{nl_b} = \frac{\Delta t}{\delta t} \left[\exp\left(-\frac{\Delta t}{\tau_{th}}\right) - \exp\left(-\frac{\Delta t}{\tau_{th_b}}\right) \right] \quad (6)$$

To maximize ΔR_{nl} , the key laser pulse width Δt_{nl} should be selected to have $\frac{\partial \Delta R_{nl}}{\partial \Delta t} = 0$, then the nonlinear ratio difference achieves maximum and provides highest sensitivity and image contrast.

To explore the laser pulse width dependent characteristics of the nonlinear ratio, a set of simulations are performed by sweeping the laser pulse width with different thermal relaxation time τ_{th} . Fig 2(a) shows that with larger τ_{th} , the amplitude of the nonlinear ratio R_{nl} increases

significantly due to better thermal confinement capability of the target. Meanwhile, the key pulse width $\Delta t_k = \tau_{th}$ also increases for maximum nonlinear ratio value. On the other hand, when we fix the thermal relaxation time of the target to be 50 μs and sweep τ_{th_b} , from Fig. 2(b) we observe that with larger τ_{th_b} (smaller difference between target and background), the amplitude of nonlinear ratio difference ΔR_{nl} decreases, but the key Δt_{nl} increases for maximum nonlinear ratio difference.

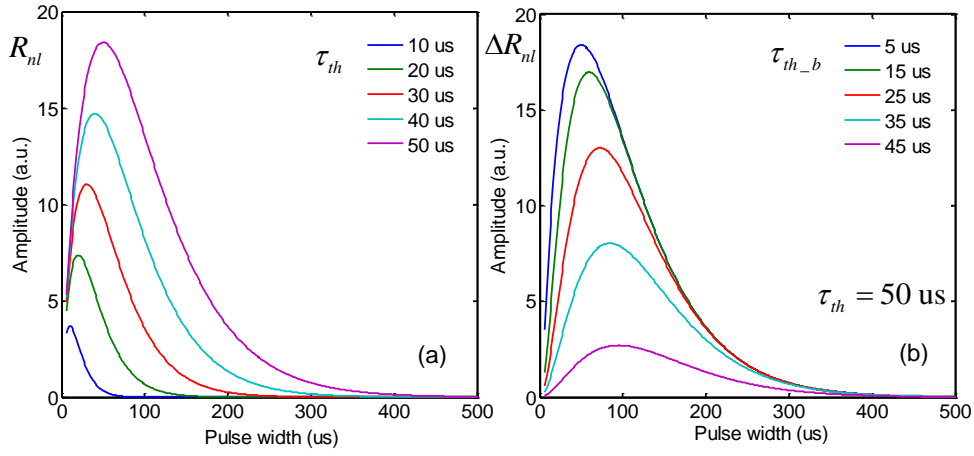


Fig. 2 (a) The amplitude of the nonlinear ratio versus laser pulse width with different thermal relaxation time of the target τ_{th} . (b) The amplitude of the nonlinear ratio difference versus laser pulse width with different thermal relaxation time of the background τ_{th_b} , while τ_{th} is fixed at 50 μs .

3) Higher pulse repetition rate under the above condition

Although there is no significant heat accumulation within single pulse under the above condition using low-power laser diode, the long-term heat accumulation and absolute temperature rising could be significant when the laser pulse repetition rate (N pulses per second) is increased. Both p_1 and p_2 will be increased linearly with pulse repetition rate due to increased absolute temperature. The Gruneison saturation term needs to be changed as Gruneisen increase term ($b\eta_{th}\mu_a\phi\Delta tN$) that is linearly proportional to the average power (pulse repetition rate) of the laser diode:

$$p_1 = (\Gamma_0 + b\eta_{th}\mu_a\phi\Delta tN)\eta_{th}\mu_a\phi\delta t \quad (7)$$

$$p_2 = (\Gamma_0 + b\eta_{th}\mu_a\phi\Delta tN)\eta_{th}\mu_a\phi \left[\delta t + \Delta t \exp\left(-\frac{\Delta t}{\tau_{th}}\right) \right] \quad (8)$$

It shows that the absolute temperature change due to the increased repetition rate of the laser source is linearly related with the signal amplitude of both p_1 and p_2 at a fixed laser pulse width. However, the nonlinear ratio between them is also constant with same expression of Eq. (5). It immediately enables the concurrent temperature detection and close-loop control during photothermal treatment [21, 22].

The experimental setup is shown in Fig. 3. The input square-wave pulse with tunable pulse width is generated by a function generator (Tektronix), which is connected to a current driver. The output of the driver is then fed to a laser diode (wavelength: 808 nm, power: 1 W) with fiber coupling. The output light from the fiber is then collimated and focused by condenser lens on the sample with spot size of 100 μm . Meanwhile, a beam splitter and photodiode are utilized to monitor the laser intensity variation. An ultrasound transducer (Doppler Inc.) with 1 MHz central frequency is placed close to the sample. Both of them are immersed in water for optimum optical and acoustic coupling. The dual PA signals are firstly amplified by a low-noise amplifier (5662, Olympus), then recorded by an oscilloscope with 100 MSPS sampling rate.

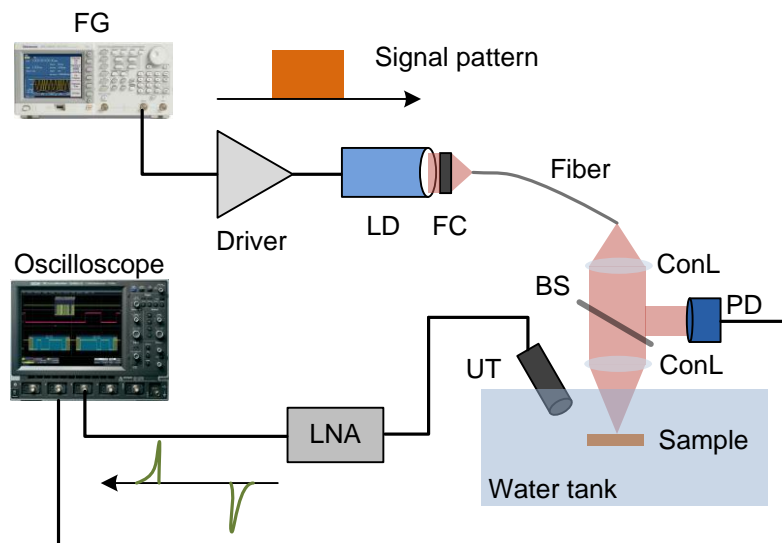


Fig. 3. The schematic of the experimental setup. FC: function generator; LD: laser diode; FC: fiber coupler; ConL: condenser lens; BS: beam splitter; PD: Photodiode UT: ultrasound transducer; LNA: low-noise amplifier.

The first observation of the LDPA nonlinear effect is from a black rubber wire sample, which has strong optical absorption at the laser's wavelength. For comparison, the conventional single PA signal could be generated by short laser pulse width. With 1 μs laser pulse width (Fig. 4(a)), only one PA signal could be generated (Fig. 4(c)). On the other hand, a typical measured waveform of LDPA signal with 10 μs laser pulse width (Fig. 4(b)) is shown in Fig. 4(d). As expected, the delay between the two PA signals generated from rising and falling edges of pulse laser illumination is also 10 μs . The waveforms of the two PA signals show high correlation and inverted amplitude, which is caused by the initial expansion (first PA signal) and contraction (second PA signal) from the same optical absorber. In addition, the peak-to-peak amplitude of the second nonlinear PA signal is larger than that of first linear PA signal, which results from the nonlinear amplitude increase when the pulse width (10 μs) is shorter than the key pulse width Δt_k , then fluence accumulation surpasses the thermal diffusion.

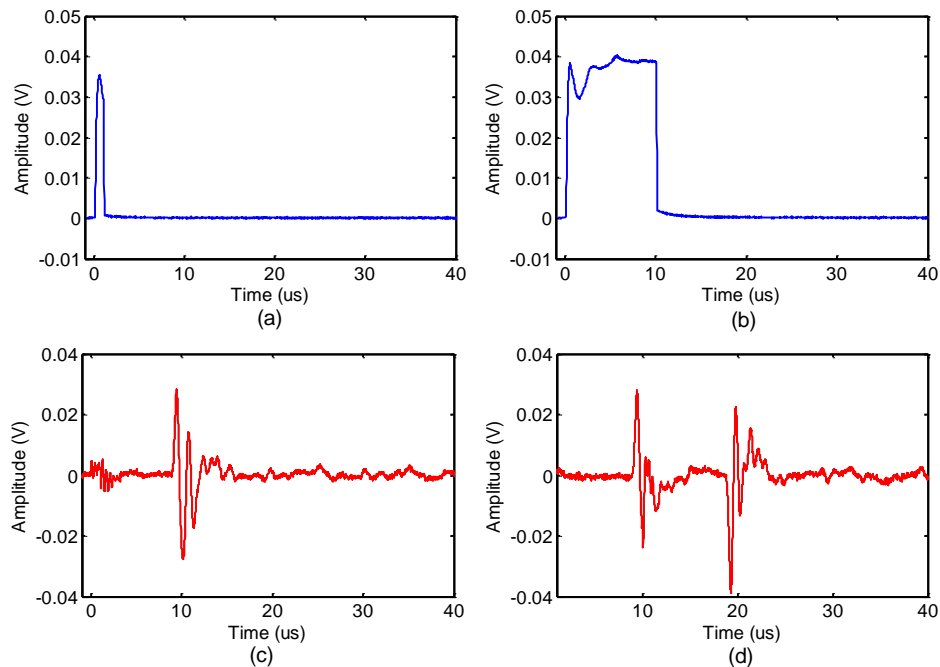


Fig. 4 (a)-(b) The light illumination signal detected by the photodiode with pulse width of 1 μs and 10 μs . (c)-(d) The measured LDPA signals with 1 μs and 10 μs pulse width laser illumination.

By sweeping the laser pulse width from 6 μs to 900 μs , the amplitudes of both first PA signal and second signals are recorded as shown in Fig. 5. As expected, the first PA signal's amplitude keeps almost constant when sweeping the laser pulse width, because the expansion-induced PA

signal is generated by the rising edge of light illumination, and not influenced by the heat accumulation and diffusion during the long-pulse light illumination. However, the second PA signal, as well as the ratio between the two PA signals, experiences an increase ($<10 \mu\text{s}$), flat ($10\sim 20 \mu\text{s}$) and decrease ($20\sim 500 \mu\text{s}$) when sweeping the laser pulse width. The measurement result agrees well with the prediction in Eq. (4). When the pulse width exceeds $500 \mu\text{s}$, the amplitude of the second PA signal begins to increase again, which may be caused by the more significant temperature rising and increased Gruneisen relaxation term in Eq. (2).

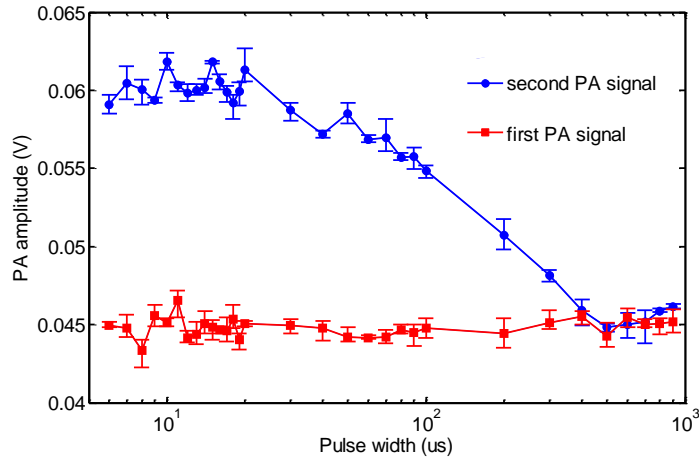


Fig. 5 Amplitudes of first PA signal (red line, square symbol) and second PA signal (blue line, circle symbol) by sweeping the pulse width of the laser source.

To explore the temperature-dependent property of the LDPA effect, the repetition rate of the laser source (fixed pulse width: $10 \mu\text{s}$, peak power: 1 W) is swept from 100 Hz to 1.9 kHz , which corresponds to average power sweeping from 1 mW to 19 mW . Fig. 6(a) shows the amplitudes of the two PA signals versus average power sweeping. As expected, with increasing average power of the laser source, absolute temperature of the sample also increases. Then the elevated Gruneisen coefficient enhances both PA signals, which is predicted from Eq. (7) and (8). On the contrary, the nonlinear ratio between the two PA signals keeps constant with varying average power (Fig. 6(b)), which is predicted from Eq. (5).

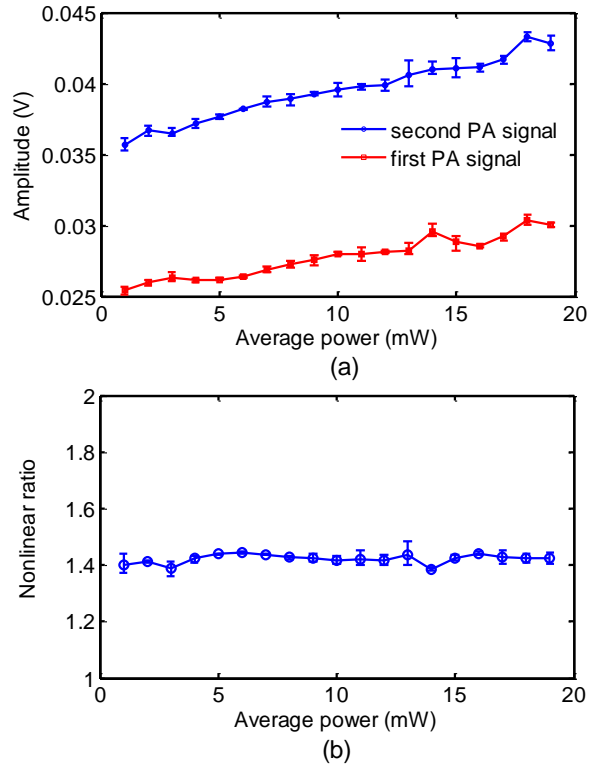


Fig. 6 (a) Amplitudes of first PA signal (red line, square symbol) and second PA signal (blue line, circle symbol) by sweeping the average power of the laser source. (b) The nonlinear ratio between the two PA signals by sweeping the average power of the laser source.

The potential applications of the proposed LDPA effect could include but not limited to:

LDPA effect for dual-contrast optical/thermal imaging: It is straightforward to enable dual-contrast imaging by utilizing the proposed LDPA effect for both optical absorption and thermal diffusivity imaging. From Eq. (1), the conventional PA imaging for absorption contrast could be achieved by mapping the amplitude of the first PA signal. Moreover from Eq. (5), the thermal diffusivity imaging could be done by mapping the nonlinear ratio between the two PA signals, which is intrinsically decoupled from optical absorption coefficient.

LDPA effect for nanoparticle-enhanced PA imaging: Although the LDPA nonlinear effect could be observed from the black rubber wire sample, the nonlinear ratio is only around 1.4, which shows that the nonlinearity of the black rubber wire is not quite significant. Compared with conventional contrast-enhanced PA imaging utilizing nanoparticles with strong optical absorption, the nanoparticles with strong thermal confinement property is preferred to enhance

the LDPA nonlinear effect. From the developed analytical model, the nanoparticles should show good thermal confinement (smaller thermal diffusivity), which may originate from single particle, and/or the conjugation of the nanoparticles to confine the laser induced heating [23].

LDPA effect for close-loop photothermal treatment and photoacoustic temperature sensing: As discussed, LDPA signal is generated from pulse-modulated CW laser and is linearly proportional to the absolute temperature of the object. On the other hand, photothermal treatment is also usually performed by CW laser. Therefore, utilizing the LDPA effect, it could immediately enable close loop photothermal treatment with PA temperature monitoring by self-regulating the repetition rate of the laser source [21].

LDPA effect for axial-resolution improvement of PA imaging: Based on the theory of Gruneisen relaxation PA microscopy [15], the proposed LDPA effect is also potential to improve axial-resolution of PA imaging. The subtraction of the two PA signals will render a narrower axial full width at half maximum (FWHM) due to its optical sectioning capability.

LDPA effect for PA-guided optical focusing: Using the LDPA effect for PA-guided optical focusing in scattering medium is feasible according to the reported literature [16]. Instead of utilizing two high-power pulsed lasers, comparable performance could be expected by utilizing single low-cost CW laser source based on the LDPA effect.

In conclusion, we report the LDPA nonlinear effect with one laser illumination and two PA signals detection. An analytical model is derived, and experimental validation is performed to demonstrate the feasibility of the technique. The proposed LDPA technique enables several interesting applications based on low-power low-cost laser diode, which will be further explored in future work.

Reference

- [1]. V. Ntziachristos, J. Ripoll, L. H. V. Wang, and R. Weissleder, "Looking and listening to light: the evolution of whole-body photonic imaging," *Nature Biotechnology* **23**, 313-320 (2005).
- [2]. A. C. Tam, "APPLICATIONS OF PHOTOACOUSTIC SENSING TECHNIQUES," *Reviews Of Modern Physics* **58**, 381-431 (1986).
- [3]. L. V. Wang, "Multiscale photoacoustic microscopy and computed tomography," *Nature Photonics* **3**, 503-509 (2009).
- [4]. L. V. Wang and S. Hu, "Photoacoustic Tomography: In Vivo Imaging from Organelles to Organs," *Science* **335**, 1458-1462 (2012).
- [5]. X. D. Wang, Y. J. Pang, G. Ku, X. Y. Xie, G. Stoica, and L. H. V. Wang, "Noninvasive laser-induced photoacoustic tomography for structural and functional in vivo imaging of the brain," *Nature Biotechnology* **21**, 803-806 (2003).
- [6]. M. H. Xu and L. H. V. Wang, "Photoacoustic imaging in biomedicine," *Rev. Sci. Instrum.* **77**(2006).
- [7]. H. F. Zhang, K. Maslov, G. Stoica, and L. V. Wang, "Functional photoacoustic microscopy for high-resolution and noninvasive in vivo imaging," *Nature Biotechnology* **24**, 848-851 (2006).
- [8]. F. Gao, X. Feng, and Y. Zheng, "Photoacoustic phasoscopy super-contrast imaging," *Applied Physics Letters* **104**(2014).
- [9]. F. Gao, X. Feng, and Y. Zheng, "Photoacoustic elastic oscillation and characterization," *Optics express* **23**, 20617-20628 (2015).
- [10]. F. Gao, X. H. Feng, and Y. J. Zheng, "Coherent Photoacoustic-Ultrasound Correlation and Imaging," *IEEE Trans. Biomed. Eng.* **61**, 2507-2512 (2014).
- [11]. F. Gao, Y. H. Ong, G. Li, X. Feng, Q. Liu, and Y. Zheng, "Fast photoacoustic-guided depth-resolved Raman spectroscopy: a feasibility study," *Optics letters* **40**, 3568-3571 (2015).
- [12]. A. Prost, F. Poisson, and E. Bossy, "Photoacoustic generation by a gold nanosphere: From linear to nonlinear thermoelastics in the long-pulse illumination regime," *Physical Review B* **92**(2015).
- [13]. O. Simandoux, A. Prost, J. Gateau, and E. Bossy, "Influence of nanoscale temperature rises on photoacoustic generation: Discrimination between optical absorbers based on thermal nonlinearity at high frequency," *Photoacoustics* **3**, 20-25 (2015).
- [14]. V. P. Zharov, "Ultrasharp nonlinear photothermal and photoacoustic resonances and holes beyond the spectral limit," *Nature Photonics* **5**, 110-116 (2011).
- [15]. L. Wang, C. Zhang, and L. V. Wang, "Grüneisen Relaxation Photoacoustic Microscopy," *Physical Review Letters* **113**(2014).
- [16]. P. Lai, L. Wang, J. W. Tay, and L. V. Wang, "Photoacoustically guided wavefront shaping for enhanced optical focusing in scattering media," *Nature Photonics* **9**, 126-132 (2015).
- [17]. M. A. Pleitez, T. Lieblein, A. Bauer, O. Hertzberg, H. von Lilienfeld-Toal, and W. Maentle, "In Vivo Noninvasive Monitoring of Glucose Concentration in Human Epidermis by Mid-Infrared Pulsed Photoacoustic Spectroscopy," *Analytical Chemistry* **85**, 1013-1020 (2013).
- [18]. H.-W. Wang, N. Chai, P. Wang, S. Hu, W. Dou, D. Umulis, L. V. Wang, M. Sturek, R. Lucht, and J.-X. Cheng, "Label-Free Bond-Selective Imaging by Listening to Vibrationally Excited Molecules," *Physical Review Letters* **106**(2011).
- [19]. E. I. Galanzha, E. V. Shashkov, T. Kelly, J.-W. Kim, L. Yang, and V. P. Zharov, "In vivo magnetic enrichment and multiplex photoacoustic detection of circulating tumour cells," *Nature Nanotechnology* **4**, 855-860 (2009).
- [20]. K. Wilson, K. Homan, and S. Emelianov, "Biomedical photoacoustics beyond thermal expansion using triggered nanodroplet vaporization for contrast-enhanced imaging," *Nature communications* **3**(2012).
- [21]. X. Feng, F. Gao, C. Xu, L. Gaoming, and Y. Zheng, "Self temperature regulation of photothermal therapy by laser-shared photoacoustic feedback," *Optics letters* **40**, 4492-4495 (2015).

ArXiv preprint version

- [22]. X. Feng, F. Gao, and Y. Zheng, "Photoacoustic-Based-Close-Loop Temperature Control for Nanoparticle Hyperthermia," *IEEE Trans. Biomed. Eng.* **62**, 1728-1737 (2015).
- [23]. S. Y. Nam, L. M. Ricles, L. J. Suggs, and S. Y. Emelianov, "Nonlinear photoacoustic signal increase from endocytosis of gold nanoparticles," *Optics letters* **37**, 4708-4710 (2012).

Author Contributions

Fei Gao conceived the idea, derived the analytical model and initiated the experiments. Xiaohua Feng designed the pulse-width-tunable laser diode system, contributed in the discussion, experimentation and analysis. Yuanjin Zheng supervised the whole project.